Molecular Therapy
Nucleic Acids
Original Article

Interference of DNAJB6/MRJ Isoform Switch by Morpholino Inhibits Replication of HIV-1 and RSV

Shih-Han Ko,[1,2] Yi-Jen Liau,[2] Ya-Hui Chi,[3] Mei-Ju Lai,[2] Yu-Ping Chiang,[2] Chun-Yi Lu,[2] Luan-Yin Chang,[2] Woan-Yuh Tarn,[4] and Li-Min Huang[2]

[1]Institute of Clinical Medicine, National Taiwan University College of Medicine, Taipei, Taiwan; [2]Department of Pediatrics, National Taiwan University Children's Hospital, National Taiwan University College of Medicine, Taipei 10002, Taiwan; [3]Institute of Biotechnology and Pharmaceutical Research, National Health Research Institutes, Zhunan, Taiwan; [4]Institute of Biomedical Sciences, Academia Sinica, Taipei 11529, Taiwan

The molecular chaperon MRJ (DNAJB6) exhibits two splice isoforms that have different roles in human viral infection, but the regulatory mechanism of MRJ isoform expression is yet unclear. In this study, we show that reduction of the polyadenylation factor CstF64 was correlated with the increase of the MRJ large isoform (MRJ-L) in human macrophages and elucidate the mechanism underlying CstF64-modulated MRJ isoform expression. Moreover, we exploited an antisense strategy targeting MRJ-L for virus replication. A morpholino oligonucleotide complementary to the 5′ splice site of *MRJ* intron 8 downregulated MRJ-L expression and suppressed the replication of not only HIV-1 but also respiratory syncytial virus (RSV). We demonstrated that downregulation of the MRJ-L level reduced HIV-1 replication as well as the subgenomic mRNA and viral production of RSV. The present findings that two human health-threatening viruses take advantage of MRJ-L for infection suggest MRJ-L as a potential target for broad-spectrum antiviral strategy.

INTRODUCTION

Emerging and re-emerging viruses continue to threaten humans. The development of timely available antiviral agents and broad-spectrum antiviral strategies is still necessary. The current antiviral agents essentially act on specific viral gene products, such as HIV type 1 (HIV-1) protease and reverse transcriptase and hepatitis C non-structural proteins, to interfere with viral replication.[1,2] New antiviral approaches such as targeting viral-host interactions or cellular components required for viral propagation, or manipulating the host immune response, show attractive prospects for drug development.[3,4]

Heat shock proteins (Hsps) execute several housekeeping functions, including the stabilization, proper folding, and intracellular trafficking of proteins.[5] Hsps also participate in various stages of the virus life cycle, including cell entry, uncoating, replication, gene expression, encapsidation, and virion release.[6] The human DnaJ/Hsp40 family member B6 (DNAJB6) (or the mammalian relative of DnaJ, MRJ) has been implicated in a variety of viral infections, such as HIV-1/-2 and cytomegalovirus.[7–11] *MRJ* has two alternatively spliced isoforms, namely, the large isoform (*MRJ-L*) and small isoform (*MRJ-S*).[12] *MRJ-L* includes 10 exons, encoding a protein of 326 amino-acid residues. *MRJ-S* does not have the last two exons, so it lacks the carboxyl-terminal 95 residues of *MRJ-L* but retains a 10-residue sequence from intron 8 (Figure 1A). Both isoforms contain the conserved J domain and a glycine/phenylalanine (G/F) domain.[13] MRJ acts as a chaperone and may function to prevent neurodegenerative diseases and muscular dystrophy by preventing protein misfolding and aggregation.[14,15] We previously reported that individuals with a higher level of MRJ-L in macrophages are more susceptible to HIV infection.[11] MRJ-L is crucial for HIV virion production through its interaction with the accessory protein Vpr (HIV-1) or Vpx (HIV-2), which promotes nuclear entry of the pre-integration complex.[8,11] In addition, MRJ-L enhances nuclear distribution of the human cytomegalovirus primase, and its relative ratio to MRJ-S influences viral lytic replication.[10] It has also been reported that the DnaJ family members, including MRJ in conjunction with Hsp70, participate in multiple steps of the dengue viral life cycle.[16]

The expression of *MRJ* isoforms involves the alternative utilization of two terminal exons and usage of intronic polyadenylation signals (PASs). Previously, a transcriptome-wide analysis of CstF64 (alternative name CSTF2)-mediated alternative polyadenylation revealed that *MRJ* is a potential target of CstF64.[17] CstF64 is a component of the cleavage stimulation factor (CstF) complex; it promotes polyadenylation via binding to GU/U-rich sequences downstream of the PAS of pre-mRNAs. Increased expression of CstF64 during B cell differentiation promotes the use of a weaker proximal PAS in the

Received 26 June 2018; accepted 1 December 2018;
https://doi.org/10.1016/j.omtn.2018.12.001.

Correspondence: Woan-Yuh Tarn, Institute of Biomedical Sciences, Academia Sinica, 128 Academia Road, Section 2, Nankang, Taipei 11529, Taiwan.
E-mail: wtarn@ibms.sinica.edu.tw
Correspondence: Li-Min Huang, Department of Pediatrics, National Taiwan University Children's Hospital, National Taiwan University College of Medicine, 8 Chung-Shan South Road, Taipei 10002, Taiwan.
E-mail: lmhuang@ntu.edu.tw

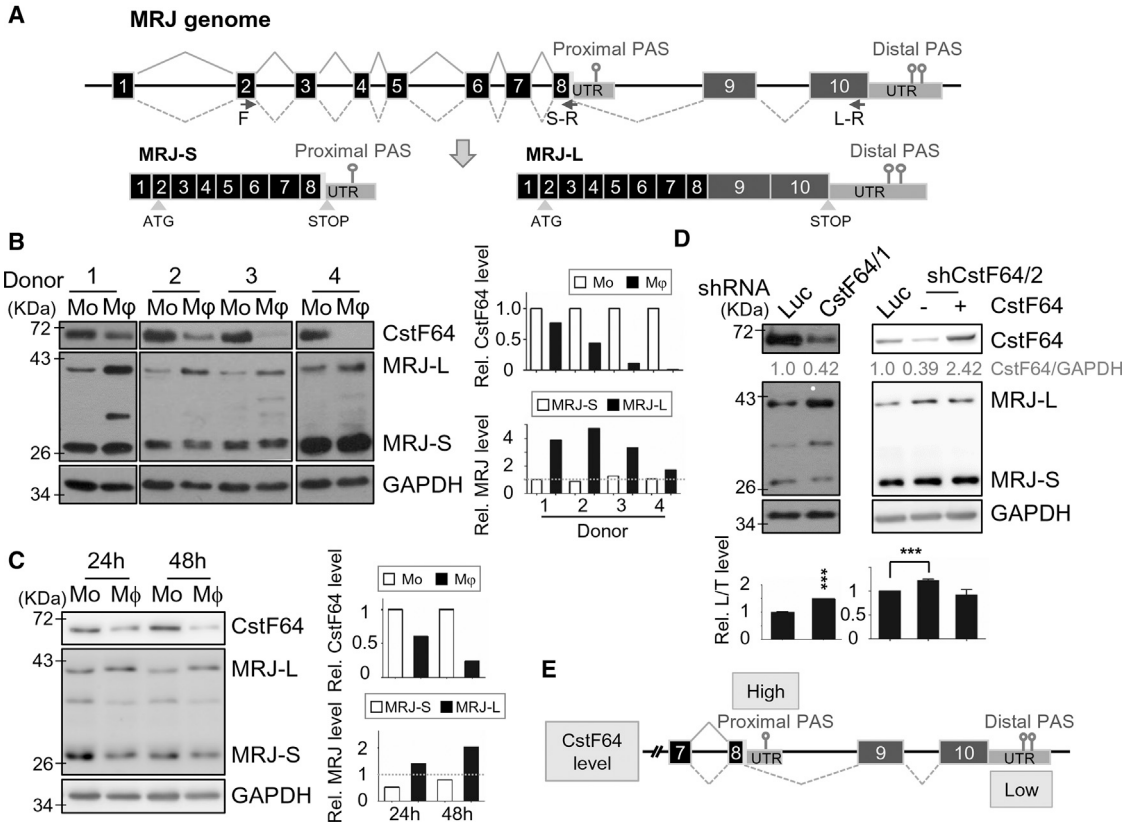

Figure 1. Expression of CstF64 and MRJ Isoforms in Monocytes and Macrophages

(A) Schematic diagram showing the *MRJ* (*DNAJB6*) gene structure and two transcript isoforms generated by alternative splicing and polyadenylation. Arrows depict the primers used for RT-PCR of *MRJ-L* or *MRJ-S* (Table S1). (B) Monocytes (Mo) collected from healthy donors were differentiated to macrophages (Mψ). Total cellular proteins were subjected to immunoblotting using antibodies against CstF64, MRJ, and GAPDH. Bar graphs indicate the levels of CstF64, MRJ-L, and MRJ-S in Mψ relative to that of Mo (set to 1); their levels were normalized to GAPDH. (C) Immunoblotting of THP-1 monocytes that were mock treated (Mo) or treated with PMA for 24 or 48 hr to differentiate into macrophage-like cells (Mψ). Antibodies used and bar graphs for relative CstF64 and MRJ levels are as described in (B). (D) THP-1 monocytes were transduced with shRNA (Luc or CstF64)-expressing lentiviruses. Immunoblotting analysis was performed using antibodies against CstF64, MRJ, and GAPDH (left panel). HEK293T cells were transduced with indicated shRNA (Luc or CstF64) and mock transformed or transformed with the CstF64 expression vector (+), followed by immunoblotting (right panel). Bar graphs indicate the ratio of MRJ-L to total MRJ (T, i.e., L+S); the data were obtained from two independent experiments. ***$p \leqslant 0.001$. (E) Schematic diagram showing that the level of CstF64 influences alternative 3′ end processing of the *MRJ* pre-mRNA. Downregulation of CstF64 promoted *MRJ-L* expression.

immunoglobulin M transcript, leading to a switch from the membrane to secretory form.[18] Nevertheless, the expression of *MRJ* isoforms also involves alternative splice-site choice, suggesting an alternative splicing-coupled polyadenylation mechanism. Therefore, a better understanding of the mechanism underlying MRJ splice-isoform expression may facilitate the development of a new antiviral strategy.

In this study, we assessed the molecular mechanism by which MRJ isoform expression is regulated in macrophages and exploited a morpholino oligonucleotide that interferes with *MRJ-L* isoform expression to block the virus life cycle. We found that MRJ-L also facilitates the replication of human respiratory syncytial virus (RSV), which is a major cause of viral bronchiolitis and pneumonia in infants and the elderly worldwide.[19] Thus, MRJ is a potential target for the development of broad-spectrum antiviral agents.

RESULTS

The Expression Level of CstF64 Is Negatively Correlated with MRJ-L in Monocytes and Macrophages

Our previous study revealed that macrophages express a higher level of MRJ-L compared with monocytes.[11] In light of the potential role of CstF64 in the polyadenylation site selection of *MRJ* mRNAs,[17] we assessed whether its expression level differs between monocytes and macrophages. CD14-positive monocytes were collected from healthy donors and induced with macrophage colony-stimulating factor (M-CSF) to differentiate into macrophages.[11] Immunoblotting revealed that macrophages had a significantly reduced level of CstF64 compared with monocytes (Figure 1B). As previously observed, two MRJ isoforms were detected.[11] The level of MRJ-L was generally increased in macrophages, whereas that of MRJ-S remained unchanged (Figure 1B). Moreover, we examined the expression of

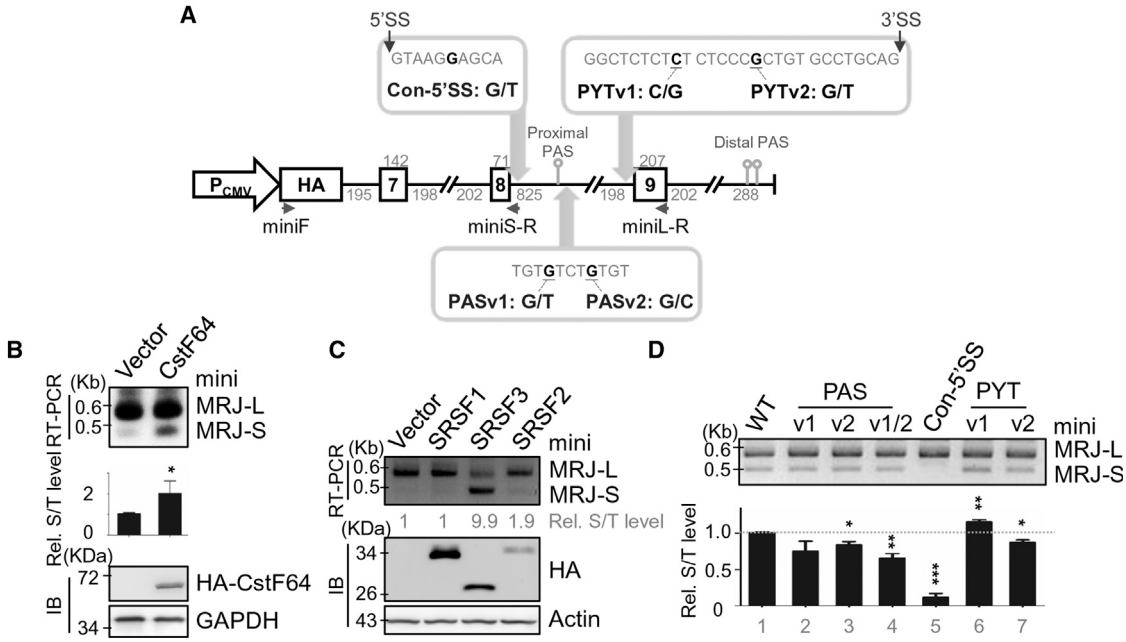

Figure 2. CstF64 Modulates Alternative 3′ End Processing of *MRJ*

(A) Diagram showing the *MRJ* minigene spanning exons 7 to 9 of the human *MRJ* gene with truncated introns. Arrows depict the primers used for RT-PCR of minigene *MRJ-L* or *MRJ-S* transcripts (Table S1), 5′ splice site (5′SS) alteration, and SNP-derived mutations that were downstream of the proximal PAS or within the polypyrimidine tract (PYT). (B) HEK293T cells were co-transfected with the *MRJ* minigene and the empty or HA-tagged CstF64-expression vector. RT-PCR was performed using the indicated primers (arrows) followed by Southern blotting (see Materials and Methods). Bar graph indicates the fold increase of minigene *MRJ-S* to total *MRJ* (T) in the CstF64 transfection. Immunoblotting (IB) was performed by using anti-HA and anti-GAPDH antibodies. (C) HEK293T cells were cotransfected with the *MRJ* minigene and the empty or expression vector encoding HA-tagged SRSF1, SRSF2, or SRSF3. Relative fold changes of minigene *MRJ-S* to total *MRJ* (T) are indicated below the gel. Immunoblotting was performed with anti-HA and anti-actin (alternative name ACTB). (D) HEK293T cells were transfected with the wild-type or mutant *MRJ* minigene vectors. Bar graph is as described in (B). For (B) and (D), mean values were obtained from three independent experiments. *$p \leqslant 0.05$; **$p \leqslant 0.01$; ***$p \leqslant 0.001$.

CstF64 and MRJ isoforms in THP-1 monocytes and macrophage-like cells differentiated from THP-1 upon phorbol myristate acetate (PMA) treatment. The result showed a decrease in CstF64 and MRJ-S and an increase in MRJ-L in PMA-induced THP-1 (Figure 1C), similar to that observed in primary cells (Figure 1B). Our result indicated that CstF64 was reduced with a concomitant switch of MRJ isoforms during monocyte differentiation into macrophages.

Next, we assessed whether CstF64, indeed, influences the expression ratio of the two MRJ isoforms. We depleted CstF64 in THP-1 cells by transducing the lentivirus expressing the *CstF64*-targeting shRNA; immunoblotting revealed that CstF64 levels were reduced to ~60% of control (Figure 1D). Under this condition, the protein level of *MRJ-S* was reduced with a concomitant increase in *MRJ-L* (Figure 1D). We also evaluated the effect of CstF64τ, a paralog of CstF64, in MRJ isoform expression. The level of MRJ-L was minimally increased when the level of CstF64τ was reduced by ~50% (Figure S1). CstF64τ may also have some, albeit minor, influence on the MRJ isoform switch. Next, we overexpressed CstF64 in CstF64-depleted HEK293T cells and observed that the MRJ-L protein level was reduced (Figure 1D). This result confirmed the role of CstF64 in the MRJ isoform switch. Together, our results indicated that CstF64 influenced the expression ratio of MRJ isoforms. Reduction of CstF64 in macrophages favored *MRJ-L* expression through the inclusion of exons 9 and 10 and the distal PAS(s) (Figure 1E).

CstF64 Modulates Alternative 3′ End Processing of the *MRJ* Transcript

To verify the role of CstF64 in *MRJ* isoform expression, we established an *MRJ* minigene reporter containing exons 7–9 with internally truncated introns (Figure 2A). The distal PAS-site-containing UTR was placed downstream of exon 9. HEK293T cells were co-transfected with the *MRJ* minigene and the hemagglutinin (HA)-tagged CstF64 expression vector. RT-PCR revealed that overexpression of CstF64 induced the expression of the minigene *MRJ-S* transcript (Figure 2B). Therefore, an elevated level of CstF64 suppressed intron 8 splicing and activated the proximal PAS within intron 8, which is in line with the aforementioned result that CstF64 depletion promoted *MRJ-L* expression.

The expression of *MRJ* isoforms is determined not only by alternative PAS selection but also by alternative usage of terminal exons. Therefore, we tested three RS-domain-containing splicing factors that can modulate splice-site selection.[20] Using the *MRJ* minigene, we observed that overexpression of SRSF3 strongly promoted *MRJ-S* expression, similar to the effect of CstF64 overexpression (Figure 2C).

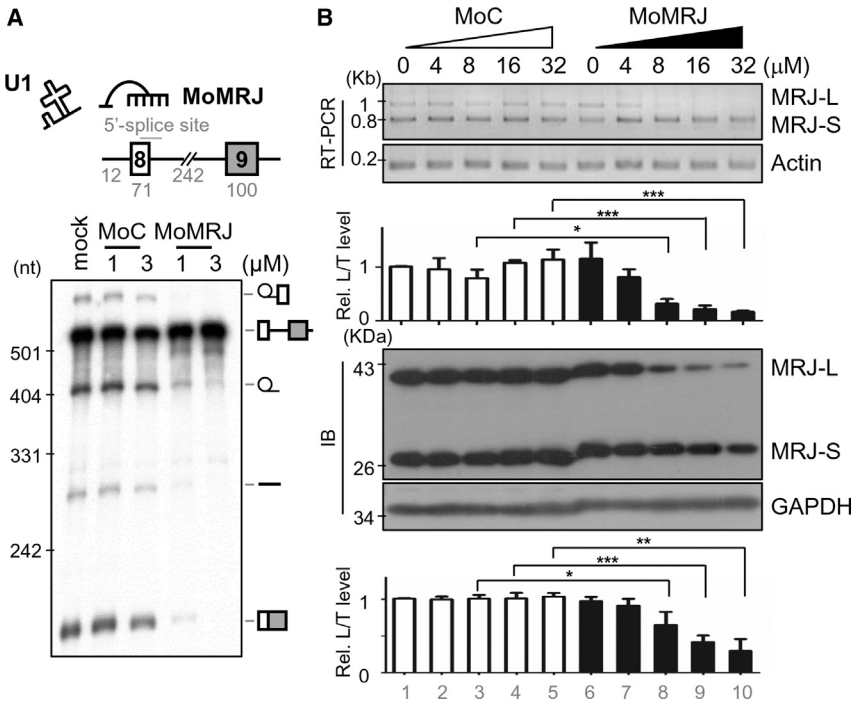

Figure 3. MoMRJ Suppresses MRJ-L Expression

(A) Diagram showing the *MRJ* pre-mRNA substrate containing exons 8 and 9 and an internally truncated intron 8. The antisense morpholino was complementary to the 5′ splice site of *MRJ* intron 8. *In vitro* splicing of ^{32}P-labeled *MRJ* pre-mRNA was performed in HeLa cell nuclear extract. MoMRJ or the negative control morpholino (MoC) was added into the reactions (mock, without morpholino). Pre-mRNA and splicing intermediates and products are depicted at the right of the gel. (B) HEK293T cells were treated with different amounts of MoMRJ or control MoC in serum-free medium for 24 hr. RT-PCR and immunoblotting were performed to determine the RNA and protein levels, respectively, of MRJ isoforms. Bar graphs indicate relative ratios of MRJ-L to total MRJ (T); data were obtained from three independent experiments. *p ⩽ 0.05; **p ⩽ 0.01; ***p ⩽ 0.001.

Perhaps, SRSF3 could suppress intron 8 splicing and/or activate the proximal PAS. Next, we evaluated the effect of SRSF3 overexpression on endogenous *MRJ* expression. Due to the difficulty of SRSF3 overexpression in THP-1 cells, we examined human epithelial type 2 (Hep2) cells and HEK293T cells. SRSF3 overexpression could increase the level of endogenous *MRJ-S* transcript in both cell lines, although the increase of MRJ-S protein was only detected in Hep2 cells (Figure S2). Therefore, SRSF3 may activate *MRJ-S* expression to various extents in different cells.

cis-Elements of the *MRJ* Gene Influence Its 3′ End Processing

We previously reported that the MRJ isoform ratio influences an individual's susceptibility to HIV-1 infection.[11] We thus examined whether SNPs exist in the splice site of the human *MRJ* gene. A search of the International Genome Sample Resource (IGSR) database[21] revealed nucleotide variations in the GT-rich region that is ~50 bases downstream of the proximal PAS (rs140379158: PASv1; rs545553573: PASv2) and the polypyrimidine tract (PYT) of intron 8 (rs528258385: PYTv1; rs192981897: PYTv2) (Figure 2A). We accordingly generated several mutant *MRJ* minigenes and evaluated isoform expression in HEK293T cells (Figure 2A, PAS and PYT mutants). First, we suspected that the two PAS mutations disrupt the GU-rich stimulatory element, which is necessary for efficient cleavage and polyadenylation;[22] hence, the two mutations would disfavor *MRJ-S* expression. The *in vivo* splicing assay, indeed, revealed that the relative level of *MRJ-S* to total *MRJ* was slightly reduced in either PAS mutant and more significantly in the double mutant (Figure 2D, lanes 2–4). Second, the two PYT mutations may interrupt (v1) or strengthen (v2) the CT-rich PYT. As expected, PYTv1 slightly increased the level of *MRJ-S*, whereas PYTv2 reduced the level of *MRJ-S* (Figure 2D, lanes 6 and 7). Moreover, we suspected that the suboptimal 5′ splice site (5′SS) of intron 8 also accounts for poor splicing and, hence, increases the probability of *MRJ-S* expression. Therefore, we changed this 5′SS to match the consensus (Figure 2A, Con-5′SS). As predicted, the improved 5′SS drastically enhanced intron 8 splicing so that only *MRJ-L* was detected (Figure 2D, lane 5). Together, our results indicated that *MRJ* isoform expression may be modulated by both polyadenylation and splicing factors, as well as by the strength of the proximal PAS and intron 8 splice sites. Although SNPs had only marginal effects on the *MRJ* isoform switch in these analyses, they may potentially impact the susceptibility to viral infection.

A Morpholino Oligonucleotide Modulates *MRJ* Splicing

We have previously shown that HIV replication was compromised by the depletion of MRJ-L using shRNA.[11] The aforementioned result indicated that the expression of MRJ-L relies on activation of intron 8 splicing (Figure 2). We thus took advantage of an octaguanidine dendrimer-conjugated morpholino oligonucleotide (namely, vivo-morpholino; hereinafter abbreviated as morpholino) to suppress MRJ-L expression. The morpholino MoMRJ was complementary to the 5′SS of intron 8 to interfere with its splicing. We evaluated the efficacy of MoMRJ using an *in vitro* splicing assay. The pre-mRNA contained *MRJ* exons 8 and 9 with an internally truncated intron (Figure 3A, upper panel). The *MRJ* pre-mRNA was spliced in HeLa nuclear extract. MoMRJ inhibited splicing, whereas the negative-control morpholino (MoC) had no effect (Figure 3A, lower panel). This result indicated that MoMRJ specifically interfered with intron 8 splicing. Next, we assessed the effect of MoMRJ on MRJ isoform expression in HEK293T cells. RT-PCR and immunoblotting revealed that increasing the amount of MoMRJ inhibited the inclusion of exons 9–10, thus reducing the expression of MRJ-L mRNA and protein (Figure 3B, lanes 7–10); MoC did not affect the MRJ ratio (lanes 2–5). Thus, MoMRJ may have the potential to interfere with MRJ-L function in cells.

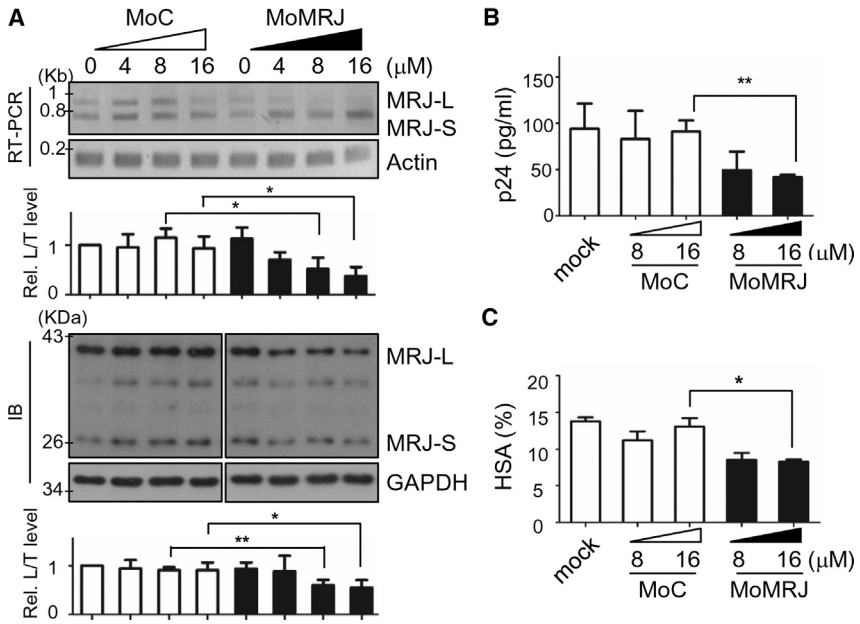

Figure 4. MoMRJ Suppresses HIV-1 Viral Replication

(A) THP-1 cells were cultured in the presence of 160 nM PMA (phorbol 12-myristate 13-acetate) for 24 hr to differentiate into macrophages, followed by treatment with MoMRJ or control MoC in serum-free medium for 24 hr. RT-PCR, immunoblotting, and quantification were performed to detect MRJ isoforms as described for Figure 3B. (B) THP-1-derived macrophages were cultured and treated with morpholinos as in (A), followed by infection with wild-type HIV-1. The viral p24 Gag protein in culture supernatants was detected by ELISA. Mean values of p24 concentration were obtained from two independent experiments. (C) Cells were cultured and treated as in (B), followed by infection with murine heat-stable antigen CD24 (HSA) of the VSV-G pseudotype HIV-1 NL4-3. Fluorescence-activated cell sorting using phycoerythrin-labeled anti-HSA was performed. Percentages of HSA representing HIV-1-positive cells were obtained from two independent experiments. *$p \leq 0.05$; **$p \leq 0.01$.

MoMRJ Inhibits HIV-1 Replication

We next examined whether MoMRJ could suppress HIV-1 replication in macrophages. As observed in HEK293T cells, MoMRJ, but not MoC, reduced MRJ-L mRNA and protein expression in THP-1 cells (Figure 4A). We treated HIV-1-infected macrophages that were derived from THP-1[23] with MoMRJ and evaluated the expression of the HIV core protein p24. The immunosorbent assay revealed that MoMRJ, but not MoC, considerably reduced the level of p24 in the medium of HIV-1-infected cells (Figure 4B). We also assessed the effect of MoMRJ in the early stage of HIV-1 infection, using a one-round infection system in which the vesicular stomatitis virus glycoprotein (VSV-G)-pseudotyped HIV-1 NL4-3 strain containing the murine heat-stable antigen CD24 (HSA) gene in the *nef* region was used as the reporter.[24] We evaluated the HSA-positive cells with fluorescence-activated cell sorting. MoMRJ reduced the number of HSA-presenting cells, whereas MoC had no significant effect (Figure 4C). This result indicated that MoMRJ could disrupt the HIV-1 life cycle during the early stage by reducing MRJ-L expression.

MRJ-L Is Essential for RSV Infection and mRNA Production

In addition to HIV-1, we further tested the effect of MRJ-L reduction in other viral infections, including one RNA virus (RSV) and two DNA viruses (adenovirus and herpes simplex virus [HSV]). RSV and adenovirus are common respiratory pathogens for humans, yet effective antiviral agents for both are lacking. Adenovirus and HSV are DNA viruses and replicate in the nucleus, whereas RSV is a single-stranded RNA virus that replicates in the cytoplasm. Using lentivirus-mediated transduction of Hep2 cells with the *MRJ-L*-targeting shRNA, we established stable MRJ-L-depleted cells. Immunoblotting revealed a significant reduction in the MRJ-L level, whereas the MRJ-S level remained unaffected (Figure 5A, lane 3). Next, we infected MRJ-L-depleted Hep2 cells with the RSV A2 strain for 48 hr and evaluated the expression of the RSV envelope F protein, which is crucial for RSV penetration, assembly, and release from cells. RSV F expression was significantly reduced in MRJ-L-depleted Hep2 cells but not in luciferase shRNA-expressing control cells (Figure 5A, lanes 5 and 6). We also performed a plaque assay to determine RSV titer and qRT-PCR to detect the mRNA of the RSV nucleoprotein N (discussed later). RSV production was reduced in MRJ-L-depleted cells (Figure 5A, bar graphs). Depletion of MRJ-S in Hep2 cells did not affect RSV production (Figure 5B). Moreover, we generated two MRJ-L knockout clones, using CRISPR-Cas9 technology, and observed that the production of viral RNA and proteins was significantly reduced (Figure 5C, bar graph and immunoblotting, respectively). Together, these results confirmed that MRJ-L is required for RSV replication. Nevertheless, depletion of MRJ-L did not significantly affect adenovirus or HSV infection (Figure S3).

The RSV ribonucleoprotein (RNP) complex is composed of the negative-sense genomic RNA encapsidated by the nucleoprotein (N).[25] The viral RNP is essential for viral genome synthesis and subgenomic mRNA production.[26] To know how MoMRJ interferes with RSV life cycle, we infected MRJ-depleted Hep2 cells with RSV for 12 hr and examined viral mRNA production. qRT-PCR revealed that depletion of MRJ-L substantially reduced the production of the viral mRNAs encoding the nonstructural protein 1 (*NS1*), the envelope fusion protein (*F*), and the RNP component *M2-1* (Figure 5D). Furthermore, we performed a rescue experiment. Since stably expressed MRJ-L was expressed in an excess amount, we observed that viral mRNA production was proportionally increased (Figure 5E). These results suggested that MRJ-L specifically facilitates subgenomic mRNA production.

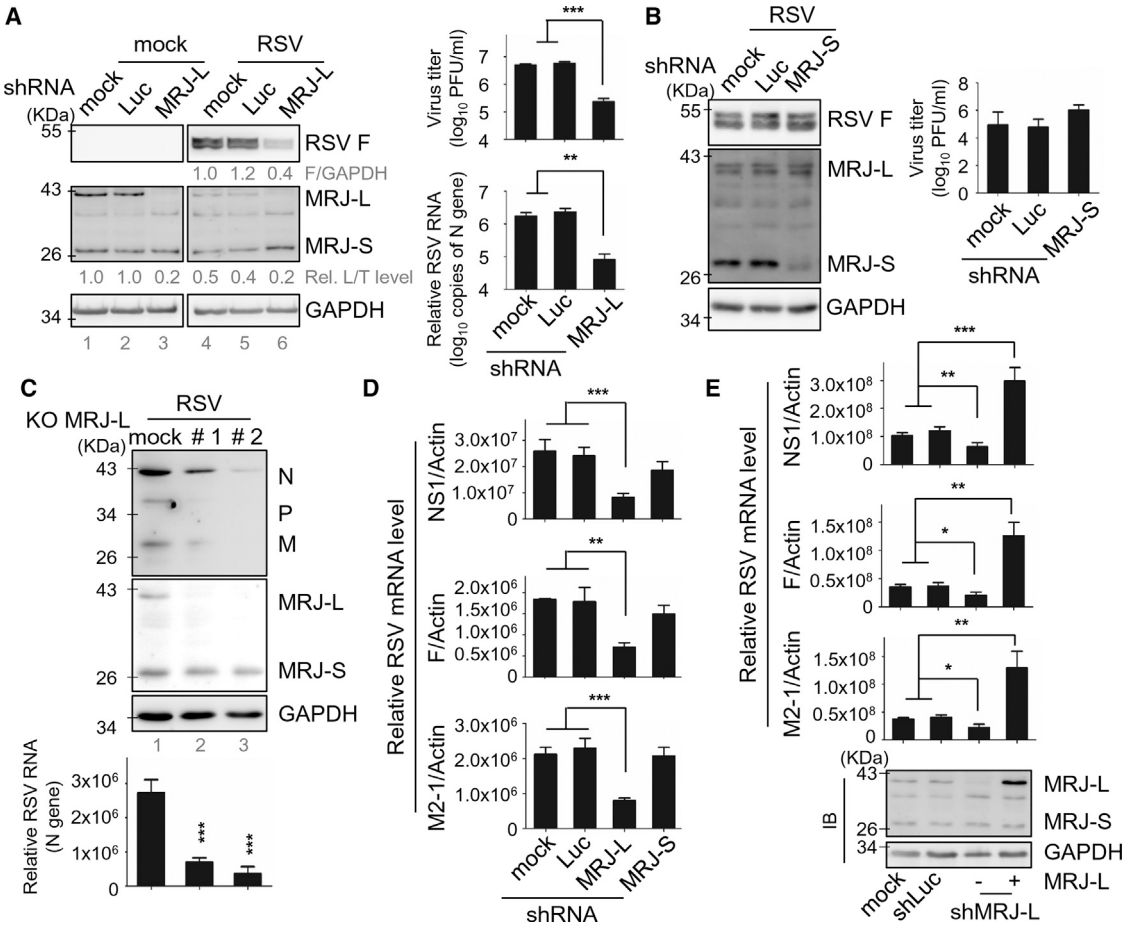

Figure 5. MRJ-L Is Essential for RSV Infection

(A) Hep2 cells were stably transduced with lentivirus expressing the control shRNA (shLuc) or shRNA-targeting *MRJ-L* (shMRJ-L), followed by infection with RSV A2 strain at an MOI of 0.1 for 48 hr. Immunoblotting was performed using antibodies against the RSV fusion protein (RSV F), MRJ, and GAPDH. The relative levels of RSV F and ratios of MRJ-L to total MRJ (T) are indicated below the respective blots. Viral titer was determined by plaque assays using culture supernatants. RSV RNA level was determined by qRT-PCR of viral nucleoprotein (*N*) transcript in the culture supernatants. (B) Hep2 cells that stably expressed shLuc or shMRJ-S were infected with the RSV A2 strain at an MOI of 0.1 for 48 hr. Immunoblotting and virus titer analysis were performed as in (A). (C) Two clones of MRJ-L-knockout Hep2 cells were infected with RSV A2 at an MOI of 0.1 for 24 hr. Immunoblotting was performed using antibodies against multiple RSV proteins (N, P, and M), MRJ, and GAPDH. Forty-four hours post-infection, the level of the viral nucleoprotein (*N*) transcript in the culture supernatants was determined by qRT-PCR. Data were obtained from two independent experiments. (D) Hep2 cells stably expressing shLuc, shMRJ-L, and shMRJ-S were infected with the RSV A2 strain at an MOI of 1 for 12 hr. The levels of viral *NS1*, *F*, and *M2-1* mRNAs were determined by RT-qPCR using specific primers (Table S2) and normalized to that of *actin*. (E) Hep2 cells were transduced with indicated shRNA (Luc or MRJ-L) and mock transformed or transformed with the MRJ-L expression vector (+). RT-qPCR was performed as in (D). Immunoblotting was performed using antibodies against MRJ and GAPDH (bottom panel). Except for (C), all of the data were obtained from three independent experiments. *$p \leqslant 0.05$; **$p \leqslant 0.01$; ***$p \leqslant 0.001$.

MoMRJ Inhibits RSV Replication

Next, we examined whether MoMRJ can constrain RSV production. We titrated MoMRJ and the control MoC in Hep2 cells. RT-PCR and immunoblotting revealed that MoMRJ efficiently reduced the mRNA and protein levels of MRJ-L but not that of MRJ-S (Figure 6A), as observed in HEK293T and THP-1 cells (Figures 3B and 4A). We then evaluated RSV infection in morpholino-treated cells; immunoblotting revealed drastically downregulated expression of RSV F protein in MoMRJ-treated cells (Figure 6B). The plaque assay and qRT-PCR of RSV nucleoprotein (*N*) mRNA confirmed that MoMRJ substantially suppressed virion production (Figure 6C). Viral subgenomic mRNA production also was reduced upon MoMRJ treatment, whereas MoC had no effect (Figure 6D). Overall, the results demonstrated that MoMRJ can suppress the replication of both HIV and RSV, which are health- or life-threatening viruses.

DISCUSSION

This study illustrates the regulatory mechanism of the *MRJ* isoform expression and the capacity of the morpholino oligonucleotide MoMRJ in viral inhibition.

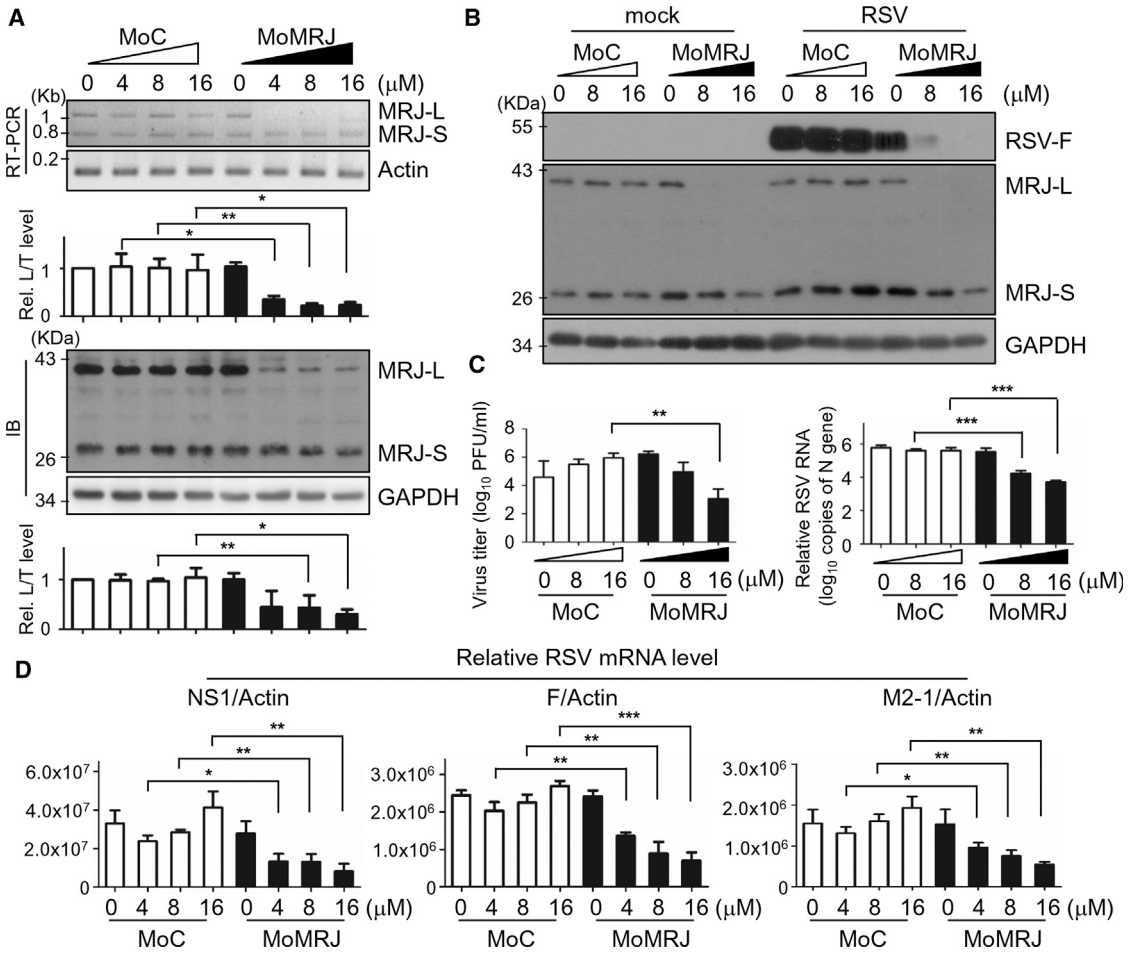

Figure 6. MoMRJ Exhibits Anti-RSV Potential

(A) Hep2 cells were treated the control MoC or MoMRJ at the indicated concentrations in serum-free medium for 24 hr. RT-PCR and immunoblotting were performed to determine MRJ RNA and protein isoforms, respectively, along with their respective controls, *actin* and GAPDH. Relative ratios of MRJ-L to total MRJ (T) were determined as in Figure 3B. (B) Hep2 cells were treated with morpholinos for 48 hr, followed by infection with the RSV A2 strain at an MOI of 0.1. Immunoblotting was performed to detect RSV F, MRJ isoforms, and GAPDH, as indicated in Figure 5A. (C) RSV titer and RNA levels were evaluated as in Figure 5A. (D) Hep2 cells were treated with morpholinos for 24 hr and subsequently infected with the RSV A2 strain at an MOI of 1 for 12 hr. Viral mRNA levels were determined as in Figure 5D. For all bar graphs, mean values were obtained from three independent experiments. *$p \leqslant 0.05$; **$p \leqslant 0.01$; ***$p \leqslant 0.001$.

Regulatory Mechanisms of MRJ Isoform Expression

Because MRJ isoforms have been individually implicated in promoting viral infection, it is necessary to understand the regulatory mechanisms underlying MRJ isoform expression. Notably, *MRJ* intron 8 is exceptionally long (24,183 nt) and has a suboptimal 5′SS, both of which are likely disadvantageous for efficient splicing. In addition, an intronic PAS located downstream of this 5′SS (at +668) may be recognized while the CstF64 level is elevated. Indeed, Yao et al.[17] reported that CstF64 associates with this proximal PAS. Moreover, our minigene analysis revealed that a strengthened 5′SS greatly promoted intron 8 splicing, resulting in *MRJ-L*, and nucleotide changes that affected the strength of the PAS or PYT of intron 8 also accordingly modulated the *MRJ* isoform ratio (Figure 2). Therefore, we deduced that a high level of CstF64 in monocytes favors *MRJ-S* production, whereas a decrease of CstF64 level in macrophages enhances *MRJ-L* production (Figure 7A). Finally, our results imply that the control of CstF64 expression is likely important for macrophage differentiation (Figure 1), as previously observed in B-lymphocyte maturation and cardiomyocyte differentiation.[27,28]

Alternative polyadenylation of *MRJ* is coupled with alternative splicing. This is reminiscent of alternative 3′ end processing of the human calcitonin/calcitonin-related peptide (*CT/CGRP*) pre-mRNA, which involves mutually exclusive usage of terminal exons and splicing-coupled alternative polyadenylation.[29] SRSF3 activates exon 4 inclusion and proximal polyadenylation of *CT/CGRP* via recognition of an intron 4 enhancer.[29] Among three SR proteins tested, SRSF3 had the greatest potential to promote *MRJ-S* expression (Figure 2). Perhaps SRSF3 may synergize the effect of CstF64 in

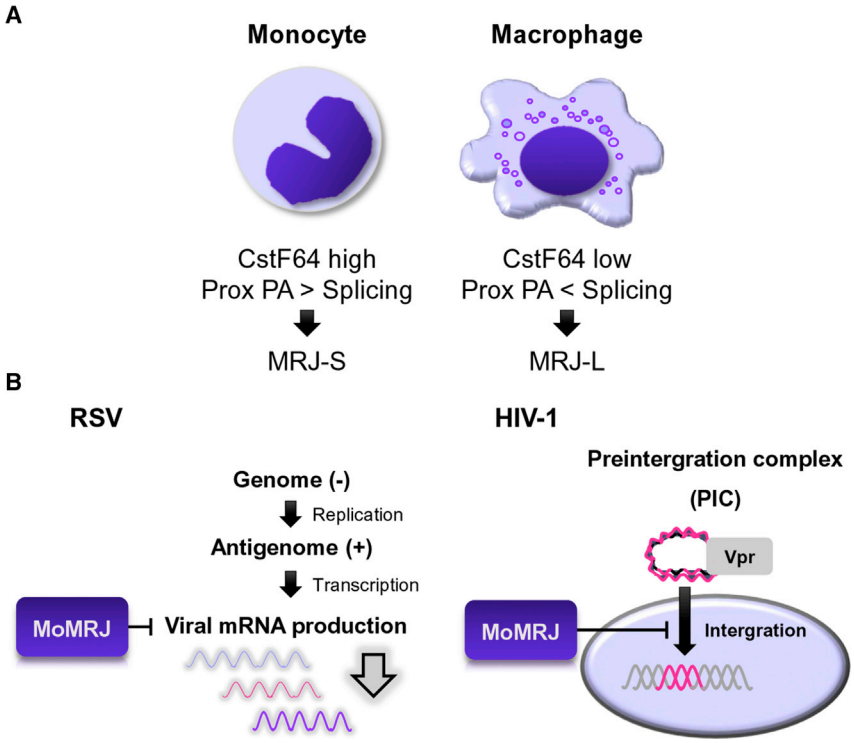

Figure 7. MRJ Isoform Expression and Antisense Morpholino against Viral Replication

(A) The upper diagram illustrates alternative splicing-coupled polyadenylation of *MRJ*, of which intron 8 is long and contains suboptimal 5′SS and PYT. A high level of CstF64 competes with the splicing machinery in intron 8 and favors *MRJ-S* production in monocytes, whereas decreased levels of CstF64 in macrophages allow splicing to take place in intron 8 and thus promote *MRJ-L* expression. Prox PA, proximal polyadenylation. (B) Diagram showing the use of an antisense morpholino for antiviral replication. Left: MoMRJ restricts RSV propagation via its limitation in subgenomic mRNA production. Right: MoMRJ suppresses HIV-1 replication via its interaction with Vpr, which is known to aid in nuclear import of the pre-integration complex (PIC).

activating the PAS in intron 8 of *MRJ*, which is similar, in part, to the scenario for *CT/CGRP*, and thus prevent splicing.

MRJ Intron Variations and Infection Susceptibility

High levels of MRJ-L increase an individual's susceptibility to HIV-1 infection.[11] SNPs of the *MRJ* gene may possibly influence its isoform ratios. The two tested PAS nucleotide variants (PASv1 and PASv2) likely compromised proximal PAS polyadenylation and thus downregulated *MRJ-S* expression (Figure 2). Variations in the PYT of intron 8 may influence the binding of the U2 auxiliary factor that is required for the binding of U2 small nuclear RNP (snRNP) to the pre-mRNA branch site. As expected, the poorer PYT (v1) reduced intron 8 splicing and thus upregulated *MRJ-S* expression, whereas the better PYT (v2) had the opposite effect (Figure 2). We speculate that individuals with PASv1, PASv2, or PYTv2 may be more vulnerable to HIV-1 infection, owing to their potential higher level of MRJ-L expression.

Antisense Morpholinos Targeting MRJ for Viral Infection

A variety of viruses take advantage of the DNAJ family to facilitate their life cycle. MRJ-L promotes nuclear entry of the HIV genome, as well as cytomegalovirus DNA synthesis.[8,10,11] In this report, we demonstrated that MRJ-L also facilitates the replication of RSV via its essential role in mRNA production (Figure 5). Besides MRJ, RSV particle assembly and maturation may also involve other Hsps such as Hsp90 and Hsp70.[30,31] In addition, two human Hsp40 (DNAJ) families—i.e., DNAJA1 and DNAJB1—facilitate replication of the Japanese encephalitis virus and influenza virus, respectively.[32,33] Therefore, targeting these chaperones may serve as a strategy for preventing viral propagation.

Antisense therapy has been used for treatment of genetic disorders or viral infections.[34] For example, antisense morpholino oligonucleotides targeting the Ebola virus VP24 gene and the Marburg virus NP gene can effectively limit viral replication.[35] Hence, broad-spectrum antiviral agents may be beneficial for combating emerging viral diseases. Our study demonstrates that MoMRJ, which interfered with *MRJ-L* expression, substantially reduced HIV replication in THP-1-derived macrophages (Figure 4) and crippled RSV amplification and production in Hep2 cells (Figure 6). Thus, MoMRJ has potential as a broad-spectrum antiviral agent or could be used as an adjuvant in conjunction with other antiviral agents (Figure 7B).

MATERIALS AND METHODS

Cell Cultures and Chemicals

HEK293T cells (ATCC, CRL-11268) and human lung epithelial A549 cells (A549; ATCC, CCL-185) were maintained in DMEM (HyClone) containing 10% fetal bovine serum (FBS; Biological Industries). Human epithelial type 2 (Hep2; ATCC, CCL-23) cells were cultured in DMEM containing Nutrient Mixture F-12 (DMEM/F-12; Thermo Fisher Scientific) supplemented with 10% FBS. African green monkey kidney (Vero) cells (ATCC, CCL-81) were maintained in Minimum Essential Medium (MEM; HyClone) containing 10% FBS. Human monocytes, THP-1 (ATCC, TIB-202), were cultured in RPMI 1640 (HyClone) supplemented with 10% FBS. THP-1 cells were differentiated into macrophage-like cells by adding 160 nM phorbol 12-myristate 13-acetate (PMA; P8139, Sigma-Aldrich) into the culture medium for 24 hr. Transfection using Lipofectamine 2000 (Invitrogen) or Viromer RED was performed according to the manufacturer's recommendations.

Plasmids

The CstF64 shRNA-expressing lentivirus vector was constructed by the insertion of annealed oligonucleotides TRCN0000153738

(5′-CCTGGCAAGAAATCTGGAAAT-3′) and TRCN0000278955 (5′-GAATTGTGGATCCGGAAATTG-3′) into pLKO.1-puro vector. TRCN0000278955 (shCstF64/1) targeted the coding sequences of *CstF64*, and TRCN0000153738 (shCstF64/2) targeted the 3′ UTR of *CstF64*. The control Luc vector (TRCN0000072243), pLKO.1-shCstF64/1, and pLKO.1-shCstF64/2 were provided by the National RNAi Core Facility, Academia Sinica, Taiwan. The shRNAs for *MRJ-L* (5′-GCGCAGATGGCTAACTGAGTA-3′) and *MRJ-S* (5′-CTGCTGCGCTTGGATAACAAGTAA-3′) were designed using InvivoGen siRNA Wizard. Recombinant lentiviruses were produced according to the protocol from the National RNAi Core Facility, Academia Sinica, Taiwan. The vectors expressing HA-tagged SR proteins (SRSF1, SRSF2, and SRSF3) were generated by insertion of each corresponding cDNA into pCDNA3.1 (Invitrogen). The cDNAs respectively encoding CstF64 and MRJ-L were PCR-amplified and subcloned into the lentiviral vector pLAS3w or pLAS5w, resulting in the CstF64 and MRJ-L expression vectors. To generate the *MRJ* minigene, human *MRJ* gene fragments including the 3′ part of intron 6-exon 7 fused with the 5′ part of intron 7, the 3′ part of intron 7-exon 8 fused with the 5′ part of intron 8 containing the proximal PAS, and the 3′ part of intron 8-exon 9 fused with the 5′ part of intron 10 containing distal PAS (GenBank: AC_000139) were obtained by PCR and then inserted into pcDNA3.1. The *MRJ* minigene was mutagenized using a PCR-based method with the primers listed in Table S1. Vector pCDNA-MRJ-e89 was generated by insertion of the *MRJ* gene fragments exon 8 to the 5′ part of intron 8 fused with the 3′ part of intron 8 to the 5′ part of exon 9 (AC_000139) into pCDNA3.1. The resulting vector spanning exons 8 to 9 of *MRJ* with an internally truncated intron 8 was then used for *in vitro* transcription to generate the *MRJ* pre-mRNA (discussed later). The sequences of the expression vectors and *MRJ* minigenes were confirmed by sequencing.

Isolation of CD4$^+$ T Lymphocytes and Primary Macrophages

$CD4^+$ T lymphocytes and $CD14^+$ monocytes were isolated from peripheral blood mononuclear cells of healthy donors using Ficoll-Paque gradient sedimentation (Amersham Pharmacia) and magnetic microbead affinity selection (Miltenyi Biotec). Monocytes that had differentiated into macrophages were cultured for 7 days in RPMI 1640 medium supplemented with 10% human AB serum (Invitrogen), 5% FBS, and 10 U/mL M-CSF (PeproTech, Rocky Hill, NJ, USA).

CRISPR-Cas9-Mediated MRJ-L Knockout Hep2 Cells

MRJ-L knockout Hep2 clones were generated by using gRNA (5′-GCGAGGACACAAACCGCGCCTGG-3′) (https://zlab.bio/guide-design-resources) targeting intron 9 of the human *MRJ* gene. The pAll-Cas9.Ppuro vector carrying the gRNA sequence was transfected into Hep2 cells using Viromer RED. After 3 days of selection with puromycin (10 μg/mL), the surviving cells were sorted and cultured for another 10–14 days. Genomic DNA of each single colony was extracted by using the MagNA Pure LC DNA Isolation Kit I (Roche Diagnostics). The intron 8-intron 9 region of *MRJ* was amplified, digested with T7 endonuclease I (T7E1, New England Biolabs), and subjected to Sanger sequencing (Figure S4).

In Vitro Splicing Assay

Radioisotope (^{32}P)-labeled *MRJ* pre-mRNA was generated by *in vitro* transcription using EcoRI-linearized pCDNA-MRJ-e89 vector and T7 polymerase (Promega). The preparation of HeLa nuclear extract and the *in vitro* splicing reaction were as described previously.[36] Morpholinos (discussed later) were added as indicated in the figure legends. Total RNA was extracted from cells using TRIzol reagent (Invitrogen) and fractionated on 6% denaturing polyacrylamide gels followed by autoradiography.

Cell Treatment with Morpholinos

Octaguanidine dendrimer-conjugated morpholino oligonucleotides (Gene Tools)[37] used in this study included MoMRJ (5′-CAGC ATCTGCTCCTTACCATTTATT-3′; Gene Tools), which is complementary to the 5′SS region of *MRJ* intron 8, and negative control MoC (5′-CCTCTTACCTCAGTTACAATTTATA-3′; Gene Tools). HEK293T, THP-1, and Hep2 cells were treated with morpholinos in serum-free medium for 24 hr.

HIV Production and Infection

To generate the VSV-G pseudotype of HIV-1 NL4-3, 2×10^6 HEK293T cells were cotransfected with the NL4-3 HSA R^+E^- vector (obtained from the NIH AIDS Reagent Program) and packaging vector pMD.G. To determine viral titers, cell culture supernatants were harvested 48 hr post-transfection and subjected to ELISA using anti-p24 Gag (PerkinElmer).[24] THP-1-derived macrophages (discussed earlier) were treated with morpholinos in the serum-free medium for 24 hr, followed by infection with HIV-1 NL4-3 (20 ng p24 per 1×10^5 cells) for 48 hr. Reporter gene expression was determined with fluorescence-activated cell sorting, using phycoerythrin-labeled monoclonal anti-mouse CD24 (HSA) (M1/69; Affymetrix eBioscience). HIV_{ADA} strain propagation and titration were carried out as described by Chiang et al. (2014).[11] THP-1-derived macrophages were treated with morpholinos as described earlier, followed by infection with HIV_{ADA} (20 ng p24 per 1×10^5 cells) for 6 days. Viral titer was determined as described earlier.

RSV Production and Infection

To propagate RSV, Hep2 cells grown to 80% confluency in 6-well plates were infected with the A2 strain and cultured in 2% FBS-containing DMEM/F-12 medium for 3–4 days. Viral titer was determined in the supernatants using the plaque assay.[38] In brief, diluted virus was added to Hep2 cells in 6-well plates for a 2-hr incubation at 37°C. After viral absorption, cells were washed with PBS and covered with the mixtures of 2% FBS-containing DMEM/F-12 medium and 0.3% agarose at 37°C in an incubator for 6 days. Knockdown cells were infected with RSV A2 at an MOI of 0.1 for 2 hr. After washing away unbound virus with PBS, cells were then incubated for 48 hr. Cell lysates were subjected to immunoblotting using an antibody against the envelope fusion protein (F) of RSV. The supernatants were harvested for plaque assays. Additionally, to evaluate the genomic RNA level, supernatant RNA was subjected to reverse transcription with random primers followed by qPCR (Roche) with specific primers for RSV nucleoprotein (*N*) (Table S2). The

expression of genes encoding *NS1*, *M2-1*, and *F* was examined in infected cells by reverse transcription with oligo(dT) primers and followed by qPCR (Roche) with specific primers (Table S2). For morpholino treatment, cells were absorbed with RSV A2 at an MOI of 0.1 for 2 hr. After washout of unbound viruses, incubation was continued for another 48 hr in the presence of morpholinos. Cell lysates and supernatants were collected for analysis as described earlier. Cells were treated with morpholinos for 24 hr in serum-free medium and then infected with RSV A2 at an MOI of 1 for 12 hr. Cell lysates were assayed for viral mRNA expression.

PCR, RT-PCR, and Southern Blotting

Total RNA was extracted from cells using TRIzol Reagent (Invitrogen) and subjected to reverse transcription using random primers or oligo(dT) and SuperScript III (Invitrogen) followed by PCR using gene-specific primers (Table S1). PCR products were separated on 2% agarose gels. For Southern blotting, PCR products were transferred onto nylon membranes (Bio-Rad), followed by hybridization with the ^{32}P-end-labeled *MRJ* exon 7 probe (5′-gatttacttcatttgggtcactaggtcacggggg-3′) overnight at room temperature. After extensive washing, the signals were detected by autoradiography.

Immunoblotting

Immunoblotting was performed as described by Chiang et al. (2014) using an enhanced chemiluminescence detection kit (Thermo Scientific).[11] Antibodies used were against the following proteins or epitopes: CstF64 (Abcam, ab72297), MRJ (Abnova, H00010049-A01), RSV F (Santa Cruz Biotechnology, sc-101362), RSV multiple proteins (Abcam, ab20745), HA (Covance, 16B12), actin (EMD Millipore, MAB1501), and GAPDH (Proteintech, 10494-1-AP). Horseradish peroxidase (HRP)-conjugated secondary antibodies included anti-mouse immunoglobulin G (IgG; SeraCare, 5210-0183) and anti-rabbit IgG (GeneTex, GTX213110-01)

Ethics Statement

The study was conducted according to the provisions of the 1975 Helsinki Declaration and was approved by the institutional review board of the National Taiwan University Hospital (NTUH-201409031RIND). All donors gave written consent before they participated in the study.

Statistical Analysis

The two-tailed Student's t test (GraphPad Prism 5 software) was used to determine the statistical significance of differences between values. ImageJ software (NIH, Bethesda, MD, USA) was used to quantify bands.

SUPPLEMENTAL INFORMATION

Supplemental Information includes four figures, two tables, and Supplemental Materials and Methods and can be found with this article online at https://doi.org/10.1016/j.omtn.2018.12.001.

AUTHOR CONTRIBUTIONS

L.-M.H. and W.-Y.T. monitored the progress of the study and designed experiments. S.-H.K., Y.-J.L., Y.-P.C., and M.-J.L. performed the experiments. All authors discussed the project. S.-H.K., L.-M.H., and W.-Y.T. prepared the manuscript.

ACKNOWLEDGMENTS

We thank Hua Lou (Case Western Reserve University) for the SRSF3 expression vector, Shin-Ru Shih (Chang Gung University) for the RSV A2 strain, and Sui-Yuan Chang (National Taiwan University) for the HSV-1 virus. We also thank the National RNAi Core Facility of Academia Sinica, Taiwan, for shRNA and CRISPR-Cas9 vectors and the Human Disease Modeling Center, College of Medicine, National Taiwan University for CRISPR-Cas9 experimental support. The work was supported by an intramural grant from the National Taiwan University to L.-M.H. and M.-R.C., an NTU-Academia Sinica grant (NTU-AS-106R104514 to L.-M.H. and W.-Y.T.), and the Ministry of Science and Technology, Taiwan (grant 103-2314-B-002-056-MY3 to L.-M.H).

REFERENCES

1. O'Connor, J., Vjecha, M.J., Phillips, A.N., Angus, B., Cooper, D., Grinsztejn, B., Lopardo, G., Das, S., Wood, R., Wilkin, A., et al.; INSIGHT START study group (2017). Effect of immediate initiation of antiretroviral therapy on risk of severe bacterial infections in HIV-positive people with CD4 cell counts of more than 500 cells per μL: secondary outcome results from a randomised controlled trial. Lancet HIV *4*, e105–e112.

2. Spengler, U. (2017). Direct antiviral agents (DAAs) - a new age in the treatment of hepatitis C virus infection. Pharmacol. Ther. *183*, 118–126.

3. Prasad, M., Ranjan, K., Brar, B., Shah, I., Lalmbe, U., Manimegalai, J., Vashisht, B., Gaury, M., Kumar, P., Khurana, S.K., et al. (2017). Virus-host interactions: new insights and advances in drug development against viral pathogens. Curr. Drug Metab. *18*, 942–970.

4. Brito, A.F., and Pinney, J.W. (2017). Protein-protein interactions in virus-host systems. Front. Microbiol. *8*, 1557.

5. Richter, K., Haslbeck, M., and Buchner, J. (2010). The heat shock response: life on the verge of death. Mol. Cell *40*, 253–266.

6. Knox, C., Luke, G.A., Blatch, G.L., and Pesce, E.R. (2011). Heat shock protein 40 (Hsp40) plays a key role in the virus life cycle. Virus Res. *160*, 15–24.

7. Kumar, M., and Mitra, D. (2005). Heat shock protein 40 is necessary for human immunodeficiency virus-1 Nef-mediated enhancement of viral gene expression and replication. J. Biol. Chem. *280*, 40041–40050.

8. Cheng, X., Belshan, M., and Ratner, L. (2008). Hsp40 facilitates nuclear import of the human immunodeficiency virus type 2 Vpx-mediated preintegration complex. J. Virol. *82*, 1229–1237.

9. Kumar, M., Rawat, P., Khan, S.Z., Dhamija, N., Chaudhary, P., Ravi, D.S., and Mitra, D. (2011). Reciprocal regulation of human immunodeficiency virus-1 gene expression and replication by heat shock proteins 40 and 70. J. Mol. Biol. *410*, 944–958.

10. Pei, Y., Fu, W., Yang, E., Shen, A., Chen, Y.C., Gong, H., Chen, J., Huang, J., Xiao, G., and Liu, F. (2012). A Hsp40 chaperone protein interacts with and modulates the cellular distribution of the primase protein of human cytomegalovirus. PLoS Pathog. *8*, e1002968.

11. Chiang, Y.P., Sheng, W.H., Shao, P.L., Chi, Y.H., Chen, Y.M., Huang, S.W., Shih, H.M., Chang, L.Y., Lu, C.Y., Chang, S.C., et al. (2014). Large isoform of mammalian relative of DnaJ is a major determinant of human susceptibility to HIV-1 infection. EBioMedicine *1*, 126–132.

12. Hanai, R., and Mashima, K. (2003). Characterization of two isoforms of a human DnaJ homologue, HSJ2. Mol. Biol. Rep. *30*, 149–153.

13. Mitra, A., Shevde, L.A., and Samant, R.S. (2009). Multi-faceted role of HSP40 in cancer. Clin. Exp. Metastasis *26*, 559–567.

14. Ruggieri, A., Saredi, S., Zanotti, S., Pasanisi, M.B., Maggi, L., and Mora, M. (2016). DNAJB6 myopathies: focused review on an emerging and expanding group of myopathies. Front. Mol. Biosci. *3*, 63.

15. Kakkar, V., Månsson, C., de Mattos, E.P., Bergink, S., van der Zwaag, M., van Waarde, M.A.W.H., Kloosterhuis, N.J., Melki, R., van Cruchten, R.T.P., Al-Karadaghi, S., et al. (2016). The S/T-rich motif in the DNAJB6 chaperone delays polyglutamine aggregation and the Onset of Disease in a mouse model. Mol. Cell *62*, 272–283.

16. Taguwa, S., Maringer, K., Li, X., Bernal-Rubio, D., Rauch, J.N., Gestwicki, J.E., Andino, R., Fernandez-Sesma, A., and Frydman, J. (2015). Defining Hsp70 subnetworks in dengue virus replication reveals key vulnerability in flavivirus infection. Cell *163*, 1108–1123.

17. Yao, C., Biesinger, J., Wan, J., Weng, L., Xing, Y., Xie, X., and Shi, Y. (2012). Transcriptome-wide analyses of CstF64-RNA interactions in global regulation of mRNA alternative polyadenylation. Proc. Natl. Acad. Sci. USA *109*, 18773–18778.

18. Takagaki, Y., and Manley, J.L. (1998). Levels of polyadenylation factor CstF-64 control IgM heavy chain mRNA accumulation and other events associated with B cell differentiation. Mol. Cell *2*, 761–771.

19. Cromer, D., van Hoek, A.J., Newall, A.T., Pollard, A.J., and Jit, M. (2017). Burden of paediatric respiratory syncytial virus disease and potential effect of different immunisation strategies: a modelling and cost-effectiveness analysis for England. Lancet Public Health *2*, e367–e374.

20. Long, J.C., and Caceres, J.F. (2009). The SR protein family of splicing factors: master regulators of gene expression. Biochem. J. *417*, 15–27.

21. Clarke, L., Fairley, S., Zheng-Bradley, X., Streeter, I., Perry, E., Lowy, E., Tassé, A.M., and Flicek, P. (2017). The International Genome Sample Resource (IGSR): a worldwide collection of genome variation incorporating the 1000 Genomes Project data. Nucleic Acids Res. *45* (D1), D854–D859.

22. Tian, B., and Manley, J.L. (2017). Alternative polyadenylation of mRNA precursors. Nat. Rev. Mol. Cell Biol. *18*, 18–30.

23. Konopka, K., and Düzgüneş, N. (2002). Expression of CD4 controls the susceptibility of THP-1 cells to infection by R5 and X4 HIV type 1 isolates. AIDS Res. Hum. Retroviruses *18*, 123–131.

24. He, J., Choe, S., Walker, R., Di Marzio, P., Morgan, D.O., and Landau, N.R. (1995). Human immunodeficiency virus type 1 viral protein R (Vpr) arrests cells in the G2 phase of the cell cycle by inhibiting p34cdc2 activity. J. Virol. *69*, 6705–6711.

25. El Omari, K., Dhaliwal, B., Ren, J., Abrescia, N.G., Lockyer, M., Powell, K.L., Hawkins, A.R., and Stammers, D.K. (2011). Structures of respiratory syncytial virus nucleocapsid protein from two crystal forms: details of potential packing interactions in the native helical form. Acta Crystallogr. Sect. F Struct. Biol. Cryst. Commun. *67*, 1179–1183.

26. Ortín, J., and Martín-Benito, J. (2015). The RNA synthesis machinery of negative-stranded RNA viruses. Virology *479-480*, 532–544.

27. Youngblood, B.A., and MacDonald, C.C. (2014). CstF-64 is necessary for endoderm differentiation resulting in cardiomyocyte defects. Stem Cell Res. (Amst.) *13* (3, Pt A), 413–421.

28. Romeo, V., Griesbach, E., and Schümperli, D. (2014). CstF64: cell cycle regulation and functional role in 3′ end processing of replication-dependent histone mRNAs. Mol. Cell. Biol. *34*, 4272–4284.

29. Lou, H., Neugebauer, K.M., Gagel, R.F., and Berget, S.M. (1998). Regulation of alternative polyadenylation by U1 snRNPs and SRp20. Mol. Cell. Biol. *18*, 4977–4985.

30. Brown, G., Rixon, H.W., Steel, J., McDonald, T.P., Pitt, A.R., Graham, S., and Sugrue, R.J. (2005). Evidence for an association between heat shock protein 70 and the respiratory syncytial virus polymerase complex within lipid-raft membranes during virus infection. Virology *338*, 69–80.

31. Radhakrishnan, A., Yeo, D., Brown, G., Myaing, M.Z., Iyer, L.R., Fleck, R., Tan, B.H., Aitken, J., Sanmun, D., Tang, K., et al. (2010). Protein analysis of purified respiratory syncytial virus particles reveals an important role for heat shock protein 90 in virus particle assembly. Mol. Cell. Proteomics *9*, 1829–1848.

32. Wang, R.Y., Huang, Y.R., Chong, K.M., Hung, C.Y., Ke, Z.L., and Chang, R.Y. (2011). DnaJ homolog Hdj2 facilitates Japanese encephalitis virus replication. Virol. J. *8*, 471.

33. Cao, M., Wei, C., Zhao, L., Wang, J., Jia, Q., Wang, X., Jin, Q., and Deng, T. (2014). DnaJA1/Hsp40 is co-opted by influenza A virus to enhance its viral RNA polymerase activity. J. Virol. *88*, 14078–14089.

34. Havens, M.A., and Hastings, M.L. (2016). Splice-switching antisense oligonucleotides as therapeutic drugs. Nucleic Acids Res. *44*, 6549–6563.

35. Iversen, P.L., Warren, T.K., Wells, J.B., Garza, N.L., Mourich, D.V., Welch, L.S., Panchal, R.G., and Bavari, S. (2012). Discovery and early development of AVI-7537 and AVI-7288 for the treatment of Ebola virus and Marburg virus infections. Viruses *4*, 2806–2830.

36. Tarn, W.Y., and Steitz, J.A. (1994). SR proteins can compensate for the loss of U1 snRNP functions in vitro. Genes Dev. *8*, 2704–2717.

37. Morcos, P.A., Li, Y., and Jiang, S. (2008). Vivo-morpholinos: a non-peptide transporter delivers morpholinos into a wide array of mouse tissues. Biotechniques *45*, 613–618.

38. McKimm-Breschkin, J.L. (2004). A simplified plaque assay for respiratory syncytial virus—direct visualization of plaques without immunostaining. J. Virol. Methods *120*, 113–117.